ACS APPLIED MATERIALS & INTERFACES

Research Article

www.acsami.org

Facile Fabrication of Lubricant-Infused Wrinkling Surface for Preventing Thrombus Formation and Infection

Shuaishuai Yuan,[†,‡] Shifang Luan,[*,†] Shunjie Yan,[†,‡] Hengchong Shi,[†] and Jinghua Yin[*,†]

[†]State Key Laboratory of Polymer Physics and Chemistry, Changchun Institute of Applied Chemistry, Chinese Academy of Sciences, Changchun 130022, People's Republic of China

[‡]University of Chinese Academy of Sciences, Beijing 100049, People's Republic of China

Supporting Information

ABSTRACT: Despite the advanced modern biotechniques, thrombosis and bacterial infection of biomedical devices remain common complications that are associated with morbidity and mortality. Most antifouling surfaces are in solid form and cannot simultaneously fulfill the requirements for antithrombosis and antibacterial efficacy. In this work, we present a facile strategy to fabricate a slippery surface. This surface is created by combining photografting polymerization with osmotically driven wrinkling that can generate a coarse morphology, and followed by infusing with fluorocarbon liquid. The lubricant-infused wrinkling slippery surface can greatly prevent protein attachment, reduce platelet adhesion, and suppress thrombus formation in vitro. Furthermore, *E. coli* and *S. aureus* attachment on the slippery surfaces is reduced by ∼98.8% and ∼96.9% after 24 h incubation, relative to poly(styrene-*b*-isobutylene-*b*-styrene) (SIBS) references. This slippery surface is biocompatible and has no toxicity to L929 cells. This surface-coating strategy that effectively reduces thrombosis and the incidence of infection will greatly decrease healthcare costs.

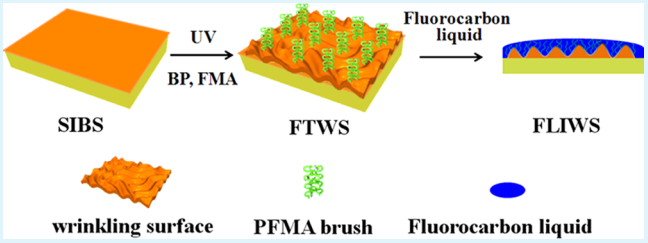

KEYWORDS: *poly(styrene-b-isobutylene-b-styrene) (SIBS), slippery surface, photografting polymerization, antifouling, antibacterial*

INTRODUCTION

As for indwelling biomedical devices, two serious problems (thrombosis and bacterial infections) are common and associated with substantial morbidity and mortality.[1−3] Thrombus formation on the surfaces of biomedical devices often requires costly device replacement or treatment with anticoagulants that increase the risk of severe complications and death.[4] Because of the growing clinical importance of biomaterial-associated infection, a series of "attacking" strategies have been proposed to actively kill bacteria.[5] These strategies involve the design of coatings or bulk materials that utilize various bactericides or drugs such as silver ions,[6] halamine,[7] cationic polymers,[8−11] antimicrobial peptides,[12] and antibiotics.[13] However, poor hemocompatibility or drug resistance is of great concern.[14]

When contacting with bloodstream, a cascade of events is initiated, e.g., protein adsorption and platelet adhesion and activation and finally result in a thrombus on a biomedical device surface.[15] The adherent proteins on the surfaces of biological implants provide a conditioning layer for bacterial attachment and subsequent biofilm formation.[16] Biofilm can in turn stimulate additional thrombus formation, therefore establishing a feedback loop that facilitates further bacterial adhesion.[17] The strong interrelationship between thrombus formation and biofilm necessitates a technology that effectively mitigates both complications.[4]

Recent advances have led to the emergence of the promising antifouling approaches that popularly utilize poly(ethylene glycol) (PEG),[18,19] poly(carboxybetaine methacrylate),[20−23] poly(sulfobetaine methacrylate),[24−27] poly(*N*-vinylpyrrolidone),[28] poly(acrylamide)s,[29,30] and neutral polysaccharides,[31] aiming at suppressing both thrombus formation and bacterial infections. Notably, stable bacterial attachment and biofouling on these traditional antifouling surfaces eventually occur because the inevitable defects in the surface chemistry serve as a nucleation site.[5]

Inspired by nature's Nepenthes pitcher plant, a slippery liquid-infused porous surface (SLIPS) was first introduced by Aizenberg and co-workers.[32] This SLIPS, which was prepared by infiltrating low-surface-energy porous Teflon membranes with lubricating liquids, provided a straightforward and versatile solution for liquid repellency and resistance to fouling. Hereafter, various strategies have been proposed to fabricate slippery surfaces with combinations of roughness, porosity, surface chemistry, and different infused liquids.[33−36] It has been well confirmed that the slippery surface had good repellency against blood cell, protein, and bacterial over a far longer time frame.[15,37] Rapid advances have led to several new strategies that introduce roughness features on smooth surfaces since the porous substrates are not abundant and commercially available; however, their complications or difficulties associated with these approaches limit their practical applications.[38−41]

In this paper, we introduce a facile strategy to fabricate a slippery surface as follows. A fluorocarbon-tethered wrinkling

Received: June 30, 2015
Accepted: August 13, 2015
Published: August 13, 2015

DOI: 10.1021/acsami.5b05865
ACS Appl. Mater. Interfaces 2015, 7, 19466−19473

surface is first prepared under UV irradiation by combining photografting polymerization with osmotically driven wrinkling,[42,43] followed by infusing with fluorocarbon liquid. The slippery surface has the following features. The affinity between the perfluorocarbon liquid and the fluorocarbon-tethered surface is much higher than that between the ambient fluid and the surface; the surface area is increased owing to the osmotically driven wrinkling, which is beneficial to the locking of the perfluorocarbon lubricating fluid. The in vitro biological response of the as-prepared surface to protein, blood, and bacteria is systematically investigated.

EXPERIMENTAL SECTION

Materials. Poly(styrene-*b*-isobutylene-*b*-styrene) (SIBS) with 30 wt % PS hard blocks was kindly provided by Kaneka Americas. 1H, 1H, 2H, 2H-Perfluorooctyl methacrylate (FMA) and perfluorodecalin were provided by J.K Scientific Ltd. Benzophenone (BP) was supplied by Peking Ruichen Chemicals (China). The Micro BCA protein assay reagent kit (AR1110) was purchased from Boster Biological Technology. Dulbecco's modified Eagle's medium (DMEM) and 0.25 wt % trypsin were purchased from Beijing Solarbio Science & Technology. Sterile filtered fetal bovine serum (FBS) was supplied by Beijing Yuanhengjinma Biotechnology. Methyl thiazolyl tetrazolium (MTT) was provided by Sigma-Aldrich. Bovine serum fibrinogen (BFg; p*I* = 5.6), fluorescein isothiocyanate-labeled bovine serum fibrinogen (FITC-labeled BFg), rhodamine B, crystal violet, Gram-negative *Escherichia coli* (*E. coli*; ATCC 25922), and Gram-postive *Staphylococcus aureus* (*S. aureus*; ATCC 6538), Luria–Bertani (LB) broth, and trypticase soy broth (TSB) were obtained from Dingguo Biotechnology Co., Ltd. Other reagents were analytical reagent grade and used as-received directly without further purification.

Preparation of Fluorocarbon-Tethered Wrinkling Surface and Fluorocarbon Liquid-infused Wrinkling Surface. For the preparation of fluorocarbon-tethered wrinkling surface (denoted as FTWS), SIBS film was cut into 2 cm × 1.5 cm pieces and ultrasonically cleaned in ethanol and doubly distilled water for 5 min in each step. A certain amount of monomer solution (20 vol % FMA, 80 vol % dimethylformamide (DMF), and 2 wt % BP) was deposited onto the SIBS films. The films were placed between two pieces of quartz plate and irradiated under a high intensity UV lamp for a predetermined time. After that, the films were washed with DMF, ethanol, and deionized water to remove residual monomer and finally dried in a vacuum oven for 24 h. The grafting density (GD) of poly(perfluorooctyl methacrylate) (PFMA) was calculated using the following equation:

$$\mathrm{GD} = \frac{W_1 - W_0}{S}$$

Here, W_0 and W_1 are the weights (μg) of the virgin and modified samples, respectively. S represents the surface area (cm^2) of the sample. Each result is an average of at least three parallel experiments. The fluorocarbon liquid-infused wrinkling surface (denoted as FLIWS) was generated through liquid perfluorodecalin imbibition into the FTWS sample.

Surface Characterization. ATR-FTIR spectra were obtained from a Fourier transform infrared spectrometer (FTIR; Bruker Vertex 70). Surface elemental compositions were examined by an X-ray photoelectron spectroscopy (XPS; VG Scientific ESCA MK II Thermo Avantage V 3.20 analyzer) with Al/K ($h\nu$ = 1486.6 eV) anode mono-X-ray source at the detection angle of 90°. The static water contact angle (SWCA) was measured on Drop Shape Analysis System (DSA; KRÜSS GMBH, Germany) by a sessile water drop method with 4 μL water drops. The repellent property of samples was determined by using a 100 μL solution of Rhodamine B dye in deionized water and tilting to 90 deg.

Protein Adsorption Test. The samples were dipped into a PBS solution containing BFg (0.1 mg/mL) at 37 °C for 1 h. Each sample was sequentially rinsed five times with fresh PBS, immersed in an aqueous solution containing 1.0 wt % SDS, and oscillated at 37 °C for 1 h to remove the adsorbed proteins from the sample. On the basis of the bicinchoninic acid (BCA) protein assay kit, the absorbance values of the SDS solution containing proteins was measured with a microplate reader (Tecan Sunrise, Swiss) and the amount of the adsorbed proteins was calculated. The reported data were the mean values of triplicate specimens for each sample.

In addition, FITC-labeled BFg was directly used to visually illustrate protein adsorption on the samples. The samples were dipped into the PBS solution containing FITC-labeled BFg (0.1 mg/mL) at 37 °C for 1 h. After rinsing with PBS, drying with a nitrogen flow, the samples were finally observed under confocal laser scanning microscopy (CLSM; LSM 700, Carl Zeiss).

Platelet Adhesion Assay. Fresh blood collected from a healthy rabbit was mixed immediately with a 3.8 wt % solution of sodium citrate at a dilution ratio of 9:1. (The experiments were carried out in accordance with the guidelines issued by the Ethical Committee of the Chinese Academy of Sciences.) The blood was centrifuged at 1000 rpm for 15 min to obtain the platelet-rich plasma (PRP). The samples were placed into cell culture plates. To equilibrate the samples, 3 mL of phosphate buffered solution (PBS, pH = 7.4) was added into each well overnight. After removing the PBS, the samples were dipped into PRP, followed by incubation at 37 °C for 1 h. The nonadhered cells were rinsed by PBS three times. Subsequently, the samples were fixed by 2.5 wt % glutaraldehyde at 4 °C for 10 h. Finally, the samples were washed with PBS three times, dehydrated with a series of ethanol/water mixtures (10, 30, 50, 70, 90, and 100 vol % ethanol), and then dried under vacuum. The surface of the sample was gold-sputtered in vacuum and observed with a field emission scanning electron microscopy (FESEM, XL 30 ESEM FEG, FEI Company).

Whole Blood Clotting Time. The anticoagulant properties of the samples were evaluated by the clotting time method using fresh rabbit blood. A volume of 60 μL of fresh blood was dropped onto the samples, followed by incubation at 37 °C for 1 h. Then 3 mL of deionized water was added to stop the reaction. The concentration of free hemoglobin in water was measured by a microplate reader at 540 nm. The relative absorbency of 60 mL of whole blood diluted by 3 mL of distilled water was assumed to be 100. The blood clotting index (BCI) of a biomaterial can be quantified by the following equation:

$$\mathrm{BCI}\ (\%) = \frac{\text{absorbency of sample solution}}{\text{absorbency of fresh blood solution}} \times 100$$

Antibacterial Assay. *E. coli* and S. aureus used for the bacterial adhesion and biofilm formation assay were cultivated in growth broth (LB for *E. coli*; TSB for S. aureus) at 37 °C for 24 h. The bacteria containing growth broth was then centrifuged at 2700 rpm for 10 min and resuspended to a concentration of about 1 × 10^8 cells/mL. Bacterial cell concentration was calculated by testing the absorbance of cell dispersions at 540 nm relative to a standard calibration curve. An optical density of 1.0 at 540 nm is equivalent to ~10^9 cells/mL.[44]

All the samples (1 cm × 1 cm) were then transferred to the 48-well plate, and *E. coli* and *S. aureus* were resuspended in 0.5% (wt/vol) glucose solution and fresh TSB growth medium, respectively. All samples were incubated with 1 mL of bacterial suspension (10^8 cells/mL) for 24 h at 37 °C. After incubation, the samples were rinsed in 2 mL of PBS at 37 °C for 5 min with shaking at 120 rpm to remove nonadherent bacteria. Then the samples were fixed with 3 vol % glutaraldehyde and dehydrating with a series of ethanol aqueous solution (10, 30, 50, 70, 90, 100 vol %), the adhered bacterial cells were observed under FESEM.

The crystal violet staining method was used to quantitatively determine the amount of the adherent bacteria for the 24 incubation samples. Briefly, the samples with adherent bacteria were stained by 0.1 wt % crystal violet for 1 h. The stained samples were then rinsed six times with distilled water, and the bound crystal violet was solubilized with 10 vol % acetic acid. Absorbance value at 590 nm of solution (100 μL) was measured with a microplate reader.

Cytotoxicity Assay. The standard methyl thiazolyl tetrazolium (MTT) assay was used to investigate the cytotoxicity of the samples.[31] DMEM supplemented with 10 vol % fetal bovine serum, 4.5 g/L

DOI: 10.1021/acsami.5b05865
ACS Appl. Mater. Interfaces 2015, 7, 19466–19473

Scheme 1. Fabrication of Fluorocarbon Liquid-Infused Wrinkling Surface

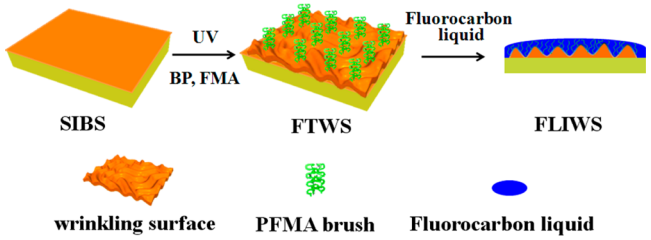

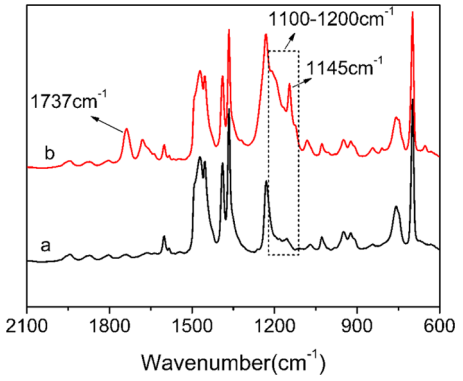

Figure 1. ATR-FTIR spectra for (a) SIBS and (b) FTWS samples.

glucose, and 100 units/mL penicillin was used to culture Murine fibroblasts cell line L929. A volume of 1 mL of medium containing the DMEM L929 fibroblasts at a density of 10^5 cells/mL were placed in each well of a 24-well plate. The plate was then incubated in a humidified 5 vol % CO_2/95 vol % air incubator at 37 °C for 24 h. The samples (1 cm × 1 cm) were gently placed on top of the cell layer in the well after replacing the medium with a fresh one. The control experiment was carried out using the growth culture medium without the samples. After incubation for another 24 h at 37 °C, the culture medium and samples in each well was removed. Culture medium (900 μL) and MTT solution (5 mg/mL in PBS, 100 μL) were then added to each well. After 4 h of incubation, the MTT solution and medium were removed and dimethyl sulfoxide (DMSO, 1 mL) was added to dissolve the formazan crystals. The optical absorbance at 490 nm was measured on a microplate reader. The results were expressed as percentages relative to the optical absorbance obtained in the control experiment.

Statistical Analysis. All data are presented as mean ± standard deviation (SD). The statistical significance was assessed by analysis of variance (ANOVA), *($p < 0.05$), **($p < 0.01$), and ***($p < 0.001$). Each result is an average of at least three parallel experiments.

RESULTS AND DISCUSSION

Styrenic thermoplastic elastomers (STPE) possess physical properties that overlap silicone rubbers and polyurethanes, and have found many biomedical applications.[45−49] As a type of popularly used STPE, SIBS has been used in various biomedical applications ranging from catheters to drug-eluting stent coatings, owing to its excellent oxidative, hydrolytic, and enzymatic stability over its lifespan in the body.[50] However, the hydrophobicity of SIBS surface may result in thrombosis and infection. As shown in Scheme 1, a fluorocarbon-tethered wrinkling structure is fabricated on the SIBS surface by combining photografting polymerization with osmotically driven wrinkling under UV irradiation. Herein, DMF solvent not only dissolves photografting FMA monomer but also simultaneously creates the wrinkling structures on the surface (Figure S1 in Supporting Information). Photografting polymerization method is used in this procedure because of its low cost, easy operation, and mild conditions.[51−53] Hereafter, perfluorodecalin liquid is infused into the FTWS sample to obtain the FLIWS sample. Perfluorodecalin liquid can be held on the FLIWS sample owing to the rough wrinkling structure and the strong van der Waals attractive force between fluorocarbon liquid and the fluorocarbon graft layer.

Surface Characterization. Photografting polymerization has another advantage that the GD of graft brush can be readily adjusted via changing photografting parameters. As shown in Figure S2 (see Supporting Information), the GD of PFMA initially increased and attained a maximum value of ~60 $\mu g/cm^2$, as photografting time elapsed. The samples that were subjected to photografting polymerization for 9 min were used in the following experiments. The chemical immobilization of PFMA onto the SIBS surface was confirmed by ATR-FTIR spectra in Figure 1, since new peaks appeared at about 1737 cm^{-1} (C═O), 1145 cm^{-1} (C−O), and 1100−1200 cm^{-1} (−C−F_2). XPS was further used to characterize surface elemental category (Figure 2) and composition (Table 1) of the SIBS and FTWS samples. A strong C_{1s} peak at ~284.6 eV and a moderate O_{1s} peak at ~532.3 eV (oxygen contamination) appeared on the SIBS sample, in

Table 1. Surface Compositions of the SIBS and FTWS Samples

	composition (at %)		
sample	C	O	F
SIBS	89.33	10.67	
FTWS	49.29	9.21	41.50

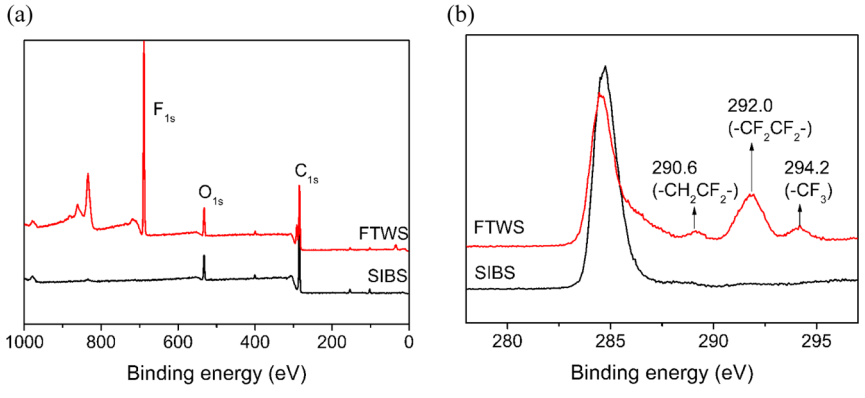

Figure 2. XPS spectra (a) and high-resolution C_{1s} spectra (b) of the SIBS and FTWS samples.

DOI: 10.1021/acsami.5b05865
ACS Appl. Mater. Interfaces 2015, 7, 19466−19473

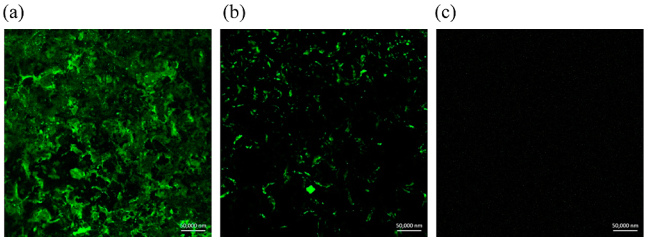

Figure 3. Representative fluorescent image of FITC-labeled fibrinogen adsorbed on (a) SIBS, (b) FTWS, and (c) FLIWS.

contrast, an additional F_{1s} peak at ~688.9 eV was obviously detected on the FTWS sample, and the F composition was up to 41.5% (Figure 2a and Table 1). To fully distinguish the functional groups on these samples, their high-resolution C_{1s} spectra were shown in Figure 2b. We found that three new peaks, i.e., $-CH_2-\underline{C}F_2-$ (at 290.6 eV), $-CF_2-\underline{C}F_2-$ (at 292.0 eV), and $-\underline{C}F_3$ (at 294.2 eV) attributing to the PFMA graft chain, appeared in the FTWS sample. The SWCA value of the SIBS sample was ~96°, while that of the FTWS samples was increased to ~127°, suggesting that the SIBS surface was almost fully covered with the PFMA graft brushes (Figure S3 in Supporting Information). A smooth fluorocarbon liquid layer was formed, which had a significant effect on the wetting properties, after infusing perfluorodecalin into the FTWS samples. The molecular smoothness interface between the test water and fluorocarbon liquid layer eliminated pinning, leading to a minimal SWCA (~69°, Figure S3c).

Suppressing Adhesion of Protein, Platelets, and Thrombosis in Vitro. Rhodamine-B aqueous solution was used to test the slippery properties of the samples, and the results are shown in Figure S4 (see Supporting Information). An obvious Rhodamine-B trail throughout the droplet sliding track was left on the SIBS surface. Also, a red droplet was observed on the FTWS surface probably due to the defects of PFMA brush. In contrast, the Rhodamine-B droplet immediately slid off the FLIWS sample, and there was nearly no evidence of any residual. It suggested that FLIWS was equally as effective as porous materials into which a large volume of fluorocarbon liquid was passively infused, in the previous SLIPS coating strategy.[32]

Material-induced thrombus is generally mediated by a combination of two different pathways that broadly grouped as humoral (involving plasma proteins) and cellular (involving platelets). Plasma protein adsorption, especially BFg, can initiate the aggregation and activation of platelet, and finally form a clot backbone.[54] Herein, CLSM was first used to visualize FITC-labeled BFg protein adsorption. It presented the strong green fluorescent image on the SIBS surface, in contrast to the weak fluorescent image on the FTWS sample and the totally dark image on the FLIWS sample (Figure 3). As tested by the BCA protein assay (Figure S5 in Supporting Information), the amount of adsorbed BFg on the SIBS surface was ~2.3 $\mu g/cm^2$. With respected to this value, the amount of adherent BFg on the FTWS and FLIWS samples were, respectively, reduced by ~50% and ~96%. The fluorinated surface with low surface energy usually resists nonspecific protein adsorption;[55] however, when the FTWS samples were exposed to protein solution for a long time, biomolecules with dynamic features passed through the fluorocarbon graft brush, finally attached to the solid surface. As for the FLIWS sample, an intact, stable lubricating film that cannot be penetrated by the protein solution is formed, therefore presenting extremely low protein attachment.

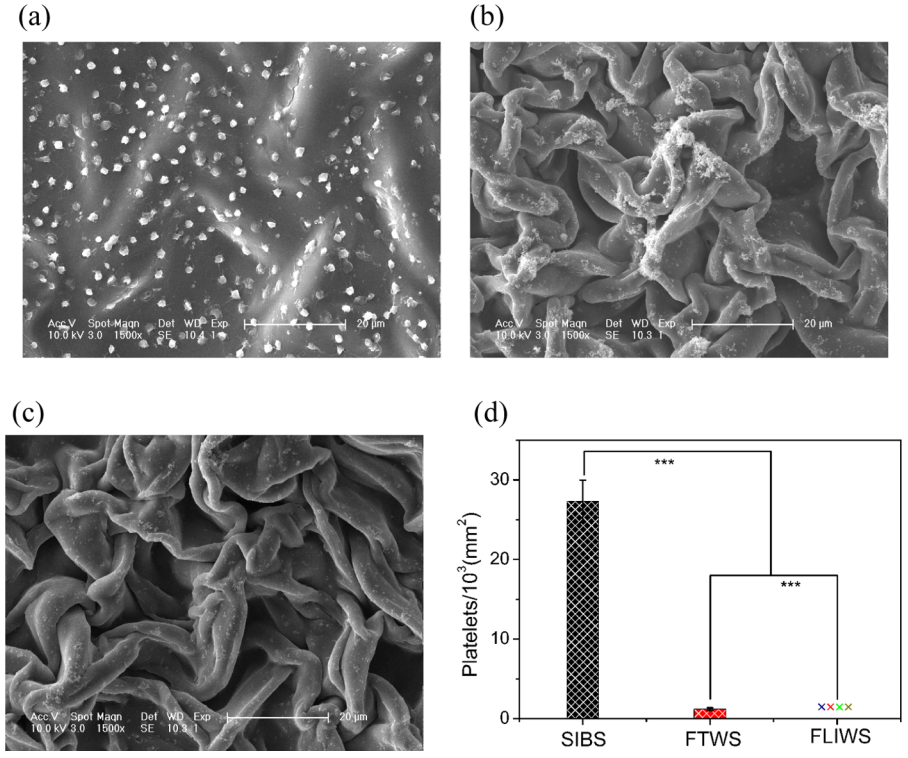

Figure 4. Representative scanning electron micrographs of (a) SIBS, (b) FTWS, and (c) FLIWS after 30 min incubation with PRP; and (d) the statistical number of the adherent platelets. Scale bar is 20 μm. Data are average cells/mm^2 from all images (error bars, standard deviations, $n = 3$). Significant difference (*$p < 0.05$; **$p < 0.01$; and ***$p < 0.001$).

DOI: 10.1021/acsami.5b05865
ACS Appl. Mater. Interfaces 2015, 7, 19466−19473

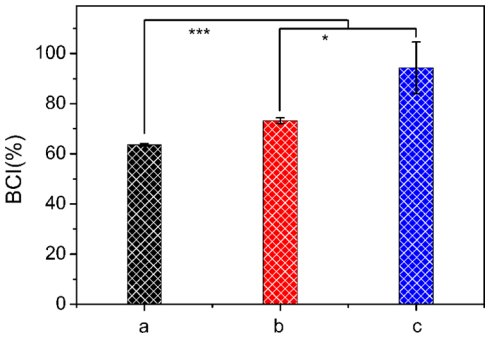

Figure 5. Blood clotting index (BCI) of (a) SIBS, (b) FTWS, and (c) FLIWS. (error bars: standard deviations, $n = 3$). Significant difference ($*p < 0.05$; $**p < 0.01$; and $***p < 0.001$).

To evaluate the platelet adhesion on the various samples, we analyzed the surfaces by FESEM after they were exposed to PRP. As shown in Figure 4, there were a large number of platelets (~2.7×10^4 per mm^2) readily adhered on the SIBS surfaces, and most of the adherent platelets were highly activated with the typical pseudopodia and spreading characteristics (Figure 4a). Just a few platelets were found on FTWS samples, and the number of adherent platelets was significantly decreased to ~1.2×10^3 per mm^2 (Figure 4b). It was in stark contrast to the SIBS and FTWS references that nearly no platelets were observed on the FLIWS surfaces (Figure 4c).

Furthermore, the clotting time was tested to assess the antithrombosis properties of the samples using fresh rabbit blood. The larger blood clotting index (BCI) means the better antithrombosis property of a surface. Among these samples, the FLIWS sample had the highest BCI with a value of ~95%, suggesting the best antithrombosis performance (Figure 5). Taken together, these results indicate that the FLIWS samples can suppress BFg adsorption, inhibit platelet adhesion, and reduce thrombosis in vitro. Notably, the FLIWS samples do not leach anticoagulant agents into blood. It potentially provides a new approach to suppress thrombosis without the complications of heparin anticoagulant.

Reduced Attachment of Bacteria. Nosocomial infection caused by medical devices is a major challenge in hospitals. To reduce nosocomial infections cases and associated hospitalization costs, it is crucial to create surfaces that resist bacterial adhesion and biofilm formation. Herein, the antibacterial activities of the samples were evaluated against two clinical pathogens *E. coli* and *S. aureus*, which are the most common species responsible for biomaterial-related infections, especially, bloodstream infection.[56] From our experimental data, a large number of *E. coli* and a thick *S. aureus* biofilm were observed on the SIBS surfaces, due to their hydrophobic property (Figure 6a). While on the FTWS surface, the number of bacteria was reduced probably because of the fluoropolymer brush (Figure 6b). However, with the passing of time, bacterial culture medium and substances secreted by bacteria could also penetrate into

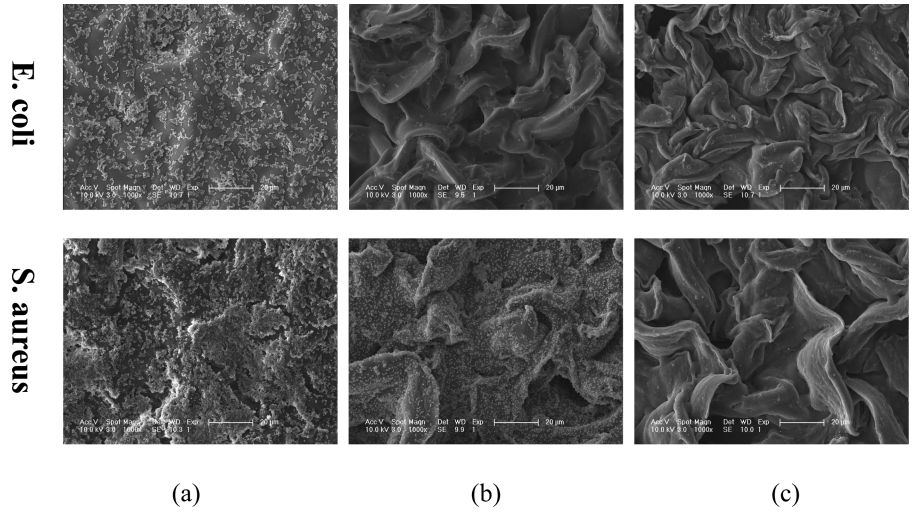

Figure 6. FESEM images of the surfaces after exposure to *E. coli* (0.5% (wt/vol) glucose; 10^8 cells/mL) and *S. aureus* (TSB; 10^8 cells/mL) for 24 h. (a) SIBS, (b) FTWS, and (c) FLIWS. Scale bar is 20 μm.

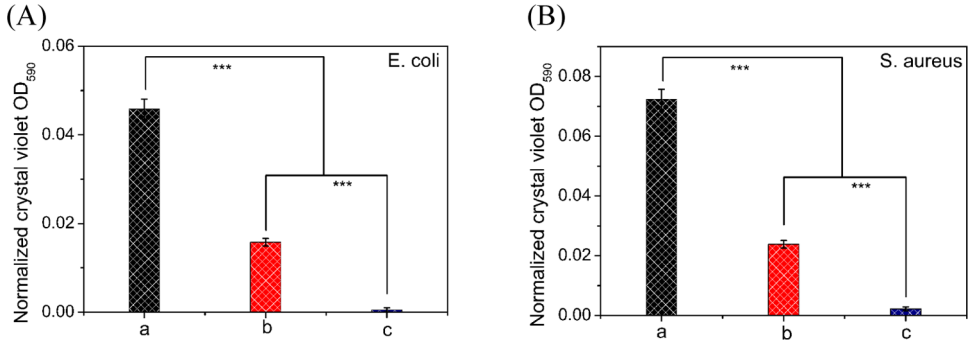

Figure 7. Crystal violet staining-based quantification of the adherent *E. coli* (A) and *S. aureus* (B) after incubation for 24 h, (a) SIBS, (b) FTWS, and (c) FLIWS. (error bars: standard deviations, $n = 3$). Significant diffrence ($*p < 0.05$; $**p < 0.01$; and $***p < 0.001$).

DOI: 10.1021/acsami.5b05865
ACS Appl. Mater. Interfaces 2015, 7, 19466−19473

the fluoropolymer graft layer, therefore masking the antifouling functionality of the FTWS sample. Because of the excellent slippery property of the intact fluorocarbon liquid layer, there were only a few sparse, isolated bacterial cells on the FLIWS sample. The antibacterial performances of the FLIWS sample were equivalent to that of SLIPS in the previous report.[15]

To quantitatively investigate the adherent bacteria, the samples after incubation were stained by crystal violet. Compared with the SIBS references, the amount of *E. coli* attachment on the FTWS and FLIWS samples were, respectively, reduced by ~65.5% and ~98.8%; as for *S. aureus*, these values were separately decreased by ~67.1% and ~96.9% (Figure 7).

Cytocompatibility Assay In Vitro. The lubricating liquid perfluorodecalin used in our experiment has been approved by the U.S. Food and Drug Administration (FDA) and widely used in biomedical fields, such as liquid ventilation, ophthalmic surgery, and blood substitutes.[15,57,58] Although perfluorodecalin has been well recognized to be nontoxic, the cytotoxicity of the samples was still evaluated with L929 cells using a MTT assay since the FLIWS samples have been subjected to the additional treatments, e.g., photografting polymerization. The viability of the L929 cells in contact with the samples for 24 h was higher than 95% in all cases, and no statistic difference in the cell viability was found among these samples (Figure 8).

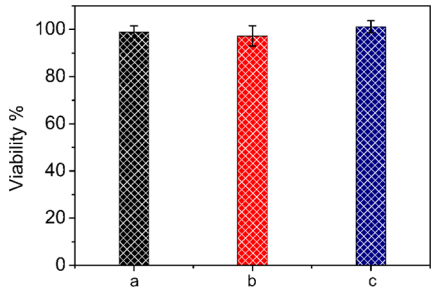

Figure 8. Viability of L929 fibroblasts on the samples of (a) SIBS, (b) FTWS, and (c) FLIWS. (error bars: standard deviations, $n = 3$).

CONCLUSION

In this work, we constructed a fluorocarbon-tethered wrinkling surface that can hold fluorocarbon liquid. The strong affinity of the lubricant to the fluorinated wrinkling surface created liquid barrier that prevent the test liquid from being exposed to the underlying solid. The lubricant-infused wrinkling slippery surface significantly inhibited protein attachment, prevents platelet adhesion, and suppresses thrombus formation in vitro. In addition, *E. coli* and *S. aureus* attachment on the slippery surfaces was greatly decreased. Notably, the slippery surface is biocompatible and has no toxicity to L929 cells. The present method could effectively suppress thrombosis while simultaneously reducing the incidence of infection without the need of antiplatelet, anticoagulant, and antibiotic drugs. The favorable antibacterial and improved hemocompatible properties as well as noncytotoxicity of the lubricant-infused wrinkling surface offer opportunities for combating infection and thrombosis of biomedical devices.

ASSOCIATED CONTENT

Supporting Information

The Supporting Information is available free of charge on the ACS Publications website at DOI: 10.1021/acsami.5b05865.

Morphology of SIBS after exposed to DMF solvent, grafting density of PFMA versus UV irradiation time, SWCA of samples, photographs of Rhodamine B-dye water before and after tilting, and BFg protein adsorption on the samples (PDF)

AUTHOR INFORMATION

Corresponding Authors

*Phone: +86 431 85262109. Fax: +86 431 85262109. E-mail: yinjh@ciac.ac.cn.

*Phone: +86 431 85262109. Fax: +86 431 85262109. E-mail: sfluan@ciac.ac.cn.

Notes

The authors declare no competing financial interest.

ACKNOWLEDGMENTS

The authors acknowledge financial support of the National Natural Science Foundation of China (Project Numbers 51473167 and 51273200), Chinese Academy of Sciences-Wego Group High-Tech Research & Development Program (Grant ZKYWG2013-01), and Scientific Development Program of Jilin Province (Grant 20130102064JC).

REFERENCES

(1) Chauhan, A.; Bernardin, A.; Mussard, W.; Kriegel, I.; Esteve, M.; Ghigo, J. M.; Beloin, C.; Semetey, V. Preventing Biofilm Formation and Associated Occlusion by Biomimetic Glycocalyxlike Polymer in Central Venous Catheters. *J. Infect. Dis.* **2014**, *210*, 1347−1356.

(2) Wu, D.; Chen, X.; Chen, T.; Ding, C.; Wu, W.; Li, J. Substrate-anchored and degradation-sensitive anti-inflammatory coatings for implant materials. *Sci. Rep.* **2015**, *5*, 11105.

(3) Chen, X.; Chen, T.; Lin, Z.; Li, X.; Wu, W.; Li, J. Choline phosphate functionalized surface: protein-resistant but cell-adhesive zwitterionic surface potential for tissue engineering. *Chem. Commun.* **2015**, *51* (3), 487−490.

(4) Smith, R. S.; Zhang, Z.; Bouchard, M.; Li, J.; Lapp, H. S.; Brotske, G. R.; Lucchino, D. L.; Weaver, D.; Roth, L. A.; Coury, A.; Biggerstaff, J.; Sukavaneshvar, S.; Langer, R.; Loose, C. Vascular Catheters with a Nonleaching Poly-Sulfobetaine Surface Modification Reduce Thrombus Formation and Microbial Attachment. *Sci. Transl. Med.* **2012**, *4*, 153ra132.

(5) Epstein, A. K.; Wong, T. S.; Belisle, R. A.; Boggs, E. M.; Aizenberg, J. Liquid-infused structured surfaces with exceptional anti-biofouling performance. *Proc. Natl. Acad. Sci. U. S. A.* **2012**, *109*, 13182−13187.

(6) Cao, Z. B.; Sun, X. B.; Yao, J. R.; Sun, Y. Y. Silver sulfadiazine-immobilized celluloses as biocompatible polymeric biocides. *J. Bioact. Compat. Polym.* **2013**, *28*, 398−409.

(7) Luo, J.; Porteous, N.; Lin, J. J.; Sun, Y. Y. Acyclic N-halamine-immobilized polyurethane: Preparation and antimicrobial and biofilm-controlling functions. *J. Bioact. Compat. Polym.* **2015**, *30*, 157−166.

(8) Petkova, P.; Francesko, A.; Fernandes, M. M.; Mendoza, E.; Perelshtein, I.; Gedanken, A.; Tzanov, T. Sonochemical Coating of Textiles with Hybrid ZnO/Chitosan Antimicrobial Nanoparticles. *ACS Appl. Mater. Interfaces* **2014**, *6*, 1164−1172.

(9) Perelshtein, I.; Ruderman, E.; Perkas, N.; Tzanov, T.; Beddow, J.; Joyce, E.; Mason, T. J.; Blanes, M.; Molla, K.; Patlolla, A.; Frenkel, A. I.; Gedanken, A. Chitosan and chitosan-ZnO-based complex nanoparticles: formation, characterization, and antibacterial activity. *J. Mater. Chem. B* **2013**, *1*, 1968−1976.

(10) Ghimire, N.; Luo, J.; Tang, R. G.; Sun, Y. Y.; Deng, Y. Novel anti-infective activities of chitosan immobilized titanium surface with enhanced osteogenic properties. *Colloids Surf., B* **2014**, *122*, 126−133.

(11) Jiang, F. G.; Yeh, C. K.; Wen, J. C.; Sun, Y. Y. N-trimethylchitosan/Alginate Layer-by-Layer Self Assembly Coatings

DOI: 10.1021/acsami.5b05865
ACS Appl. Mater. Interfaces 2015, 7, 19466−19473

Act as "Fungal Repellents" to Prevent Biofilm Formation on Healthcare Materials. *Adv. Healthcare Mater.* **2015**, *4*, 469−475.
(12) Zasloff, M. Antimicrobial peptides of multicellular organisms. *Nature* **2002**, *415*, 389−395.
(13) Aumsuwan, N.; McConnell, M. S.; Urban, M. W. Tunable Antimicrobial Polypropylene Surfaces: Simultaneous Attachment of Penicillin (Gram +) and Gentamicin (Gram -). *Biomacromolecules* **2009**, *10*, 623−629.
(14) Mi, L.; Jiang, S. Synchronizing nonfouling and antimicrobial properties in a zwitterionic hydrogel. *Biomaterials* **2012**, *33*, 8928−8933.
(15) Leslie, D. C.; Waterhouse, A.; Berthet, J. B.; Valentin, T. M.; Watters, A. L.; Jain, A.; Kim, P.; Hatton, B. D.; Nedder, A.; Donovan, K.; Super, E. H.; Howell, C.; Johnson, C. P.; Vu, T. L.; Bolgen, D. E.; Rifai, S.; Hansen, A. R.; Aizenberg, M.; Super, M.; Aizenberg, J.; Ingber, D. E. A bioinspired omniphobic surface coating on medical devices prevents thrombosis and biofouling. *Nat. Biotechnol.* **2014**, *32*, 1134−1140.
(16) Banerjee, I.; Pangule, R. C.; Kane, R. S. Antifouling Coatings: Recent Developments in the Design of Surfaces That Prevent Fouling by Proteins, Bacteria, and Marine Organisms. *Adv. Mater.* **2011**, *23*, 690−718.
(17) Boersma, R. S.; Jie, K. S. G.; Verbon, A.; van Pampus, E. C. M.; Schouten, H. C. Thrombotic and infectious complications of central venous catheters in patients with hematological malignancies. *Ann. Oncol.* **2008**, *19*, 433−442.
(18) Ma, H. W.; Hyun, J. H.; Stiller, P.; Chilkoti, A. "Non-fouling" oligo(ethylene glycol)-functionalized polymer brushes synthesized by surface-initiated atom transfer radical polymerization. *Adv. Mater.* **2004**, *16*, 338−341.
(19) Yang, W. J.; Cai, T.; Neoh, K. G.; Kang, E. T.; Teo, S. L. M.; Rittschof, D. Barnacle Cement as Surface Anchor for "Clicking" of Antifouling and Antimicrobial Polymer Brushes on Stainless Steel. *Biomacromolecules* **2013**, *14*, 2041−2051.
(20) Cheng, G.; Xue, H.; Zhang, Z.; Chen, S. F.; Jiang, S. Y. A Switchable Biocompatible Polymer Surface with Self-Sterilizing and Nonfouling Capabilities. *Angew. Chem., Int. Ed.* **2008**, *47*, 8831−8834.
(21) Cao, Z. Q.; Mi, L.; Mendiola, J.; Ella-Menye, J. R.; Zhang, L.; Xue, H.; Jiang, S. Y. Reversibly Switching the Function of a Surface between Attacking and Defending against Bacteria. *Angew. Chem., Int. Ed.* **2012**, *51*, 2602−2605.
(22) Ji, F. Q.; Lin, W. F.; Wang, Z.; Wang, L. G.; Zhang, J.; Ma, G. L.; Chen, S. F. Development of Nonstick and Drug-Loaded Wound Dressing Based on the Hydrolytic Hydrophobic Poly(carboxybetaine) Ester Analogue. *ACS Appl. Mater. Interfaces* **2013**, *5*, 10489−10494.
(23) Zhao, J.; Song, L. J.; Shi, Q.; Luan, S. F.; Yin, J. H. Antibacterial and Hemocompatibility Switchable Polypropylene Nonwoven Fabric Membrane Surface. *ACS Appl. Mater. Interfaces* **2013**, *5*, 5260−5268.
(24) Sin, M. C.; Sun, Y. M.; Chang, Y. Zwitterionic-Based Stainless Steel with Well-Defined Polysulfobetaine Brushes for General Bioadhesive Control. *ACS Appl. Mater. Interfaces* **2014**, *6*, 861−873.
(25) Jiang, S. Y.; Cao, Z. Q. Ultralow-Fouling, Functionalizable, and Hydrolyzable Zwitterionic Materials and Their Derivatives for Biological Applications. *Adv. Mater.* **2010**, *22*, 920−932.
(26) Chen, S. G.; Chen, S. J.; Jiang, S.; Xiong, M. L.; Luo, J. X.; Tang, J. N.; Ge, Z. C. Environmentally Friendly Antibacterial Cotton Textiles Finished with Siloxane Sulfopropylbetaine. *ACS Appl. Mater. Interfaces* **2011**, *3*, 1154−1162.
(27) Diaz Blanco, C.; Ortner, A.; Dimitrov, R.; Navarro, A.; Mendoza, E.; Tzanov, T. Building an Antifouling Zwitterionic Coating on Urinary Catheters Using an Enzymatically Triggered Bottom-Up Approach. *ACS Appl. Mater. Interfaces* **2014**, *6*, 11385−11393.
(28) Jiang, J. H.; Zhu, L. P.; Zhu, L. J.; Zhang, H. T.; Zhu, B. K.; Xu, Y. Y. Antifouling and Antimicrobial Polymer Membranes Based on Bioinspired Polydopamine and Strong Hydrogen-Bonded Poly(N-vinyl pyrrolidone). *ACS Appl. Mater. Interfaces* **2013**, *5*, 12895−12904.
(29) Rodriguez-Emmenegger, C.; Houska, M.; Alles, A. B.; Brynda, E. Surfaces Resistant to Fouling from Biological Fluids: Towards Bioactive Surfaces for Real Applications. *Macromol. Biosci.* **2012**, *12*, 1413−1422.
(30) Liu, Q. S.; Singh, A.; Lalani, R.; Liu, L. Y. Ultralow Fouling Polyacrylamide on Gold Surfaces via Surface-Initiated Atom Transfer Radical Polymerization. *Biomacromolecules* **2012**, *13*, 1086−1092.
(31) Li, M.; Neoh, K. G.; Kang, E. T.; Lau, T.; Chiong, E. Surface Modifi cation of Silicone with Covalently Immobilized and Cross-linked Agarose for Potential Application in the Inhibition of Infection and Omental Wrapping. *Adv. Funct. Mater.* **2014**, *24*, 1631−1643.
(32) Wong, T. S.; Kang, S. H.; Tang, S. K. Y.; Smythe, E. J.; Hatton, B. D.; Grinthal, A.; Aizenberg, J. Bioinspired self-repairing slippery surfaces with pressure-stable omniphobicity. *Nature* **2011**, *477*, 443−447.
(33) Yao, X.; Hu, Y. H.; Grinthal, A.; Wong, T. S.; Mahadevan, L.; Aizenberg, J. Adaptive fluid-infused porous films with tunable transparency and wettability. *Nat. Mater.* **2013**, *12*, 529−534.
(34) Wei, Q.; Schlaich, C.; Prevost, S.; Schulz, A.; Bottcher, C.; Gradzielski, M.; Qi, Z. H.; Haag, R.; Schalley, C. A. Supramolecular Polymers as Surface Coatings: Rapid Fabrication of Healable Superhydrophobic and Slippery Surfaces. *Adv. Mater.* **2014**, *26*, 7358−7364.
(35) Liu, H. L.; Zhang, P. C.; Liu, M. J.; Wang, S. T.; Jiang, L. Organogel-based Thin Films for Self-Cleaning on Various Surfaces. *Adv. Mater.* **2013**, *25*, 4477−4481.
(36) Glavan, A. C.; Martinez, R. V.; Subramaniam, A. B.; Yoon, H. J.; Nunes, R. M. D.; Lange, H.; Thuo, M. M.; Whitesides, G. M. Omniphobic "R-F Paper" Produced by Silanization of Paper with Fluoroalkyltrichlorosilanes. *Adv. Funct. Mater.* **2014**, *24*, 60−70.
(37) Xiao, L. L.; Li, J. S.; Mieszkin, S.; Di Fino, A.; Clare, A. S.; Callow, M. E.; Callow, J. A.; Grunze, M.; Rosenhahn, A.; Levkin, P. A. Slippery Liquid-Infused Porous Surfaces Showing Marine Antibiofouling Properties. *ACS Appl. Mater. Interfaces* **2013**, *5*, 10074−10080.
(38) Li, J. S.; Li, L. X.; Du, X.; Feng, W. Q.; Welle, A.; Trapp, O.; Grunze, M.; Hirtz, M.; Levkin, P. A. Reactive Superhydrophobic Surface and Its Photoinduced Disulfideene and Thiol-ene (Bio)-functionalization. *Nano Lett.* **2015**, *15*, 675−681.
(39) Sunny, S.; Vogel, N.; Howell, C.; Vu, T. L.; Aizenberg, J. Lubricant-Infused Nanoparticulate Coatings Assembled by Layer-by-Layer Deposition. *Adv. Funct. Mater.* **2014**, *24* (42), 6658−6667.
(40) Li, J. S.; Kleintschek, T.; Rieder, A.; Cheng, Y.; Baumbach, T.; Obst, U.; Schwartz, T.; Levkin, P. A. Hydrophobic Liquid-Infused Porous Polymer Surfaces for Antibacterial Applications. *ACS Appl. Mater. Interfaces* **2013**, *5*, 6704−6711.
(41) Howell, C.; Vu, T. L.; Lin, J. J.; Kolle, S.; Juthani, N.; Watson, E.; Weaver, J. C.; Alvarenga, J.; Aizenberg, J. Self-Replenishing Vascularized Fouling-Release Surfaces. *ACS Appl. Mater. Interfaces* **2014**, *6*, 13299−13307.
(42) Kim, H. S.; Crosby, A. J. Solvent-Responsive Surface via Wrinkling Instability. *Adv. Mater.* **2011**, *23*, 4188−4192.
(43) Chung, J. Y.; Nolte, A. J.; Stafford, C. M. Diffusion-Controlled, Self-Organized Growth of Symmetric Wrinkling Patterns. *Adv. Mater.* **2009**, *21*, 1358−1362.
(44) Yuan, S. S.; Zhao, J.; Luan, S. F.; Yan, S. J.; Zheng, W. L.; Yin, J. H. Nuclease-Functionalized Poly(Styrene-b-isobutylene-b-styrene) Surface with Anti-Infection and Tissue Integration Bifunctions. *ACS Appl. Mater. Interfaces* **2014**, *6*, 18078−18086.
(45) Lim, G. T.; Puskas, J. E.; Reneker, D. H.; Jakli, A.; Horton, W. E. Highly Hydrophobic Electrospun Fiber Mats from Polyisobutylene-Based Thermoplastic Elastomers. *Biomacromolecules* **2011**, *12*, 1795−1799.
(46) Li, X.; Luan, S.; Yuan, S.; Song, L.; Zhao, J.; Ma, J.; Shi, H.; Yang, H.; Jin, J.; Yin, J. Surface functionalization of styrenic block copolymer elastomeric biomaterials with hyaluronic acid via a "grafting to" strategy. *Colloids Surf., B* **2013**, *112*, 146−154.
(47) Puskas, J. E.; Chen, Y. H. Biomedical application of commercial polymers and novel polyisobutylene-based thermoplastic elastomers for soft tissue replacement. *Biomacromolecules* **2004**, *5*, 1141−1154.
(48) Luan, S.; Zhao, J.; Yang, H.; Shi, H.; Jin, J.; Li, X.; Liu, J.; Wang, J.; Yin, J.; Stagnaro, P. Surface modification of poly(styrene-b-

DOI: 10.1021/acsami.5b05865
ACS Appl. Mater. Interfaces 2015, 7, 19466−19473

(ethylene-co-butylene)-b-styrene) elastomer via UV-induced graft polymerization of N-vinyl pyrrolidone. *Colloids Surf., B* **2012**, *93*, 127−134.
(49) Puskas, J. E.; Chen, Y. H.; Dahman, Y.; Padavan, D. Polyisobutylene-based biomaterials. *J. Polym. Sci., Part A: Polym. Chem.* **2004**, *42*, 3091−3109.
(50) Pinchuk, L.; Wilson, G. J.; Barry, J. J.; Schoephoerster, R. T.; Parel, J. M.; Kennedy, J. P. Medical applications of poly(styrene-block-isobutylene-block-styrene) ("SIBS"). *Biomaterials* **2008**, *29*, 448−460.
(51) Edlund, U.; Kallrot, M.; Albertsson, A. C. Single-step covalent functionalization of polylactide surfaces. *J. Am. Chem. Soc.* **2005**, *127*, 8865−8871.
(52) Kallrot, M.; Edlund, U.; Albertsson, A. C. Surface functionalization of degradable polymers by covalent grafting. *Biomaterials* **2006**, *27*, 1788−1796.
(53) Tang, S. C.; Xie, J. Y.; Huang, Z. H.; Xu, F. J.; Yang, W. T. UV-Induced Grafting Processes with In Situ Formed Photomask for Micropatterning of Two-Component Biomolecules. *Langmuir* **2010**, *26*, 9905−9910.
(54) Deng, J.; Ren, T. C.; Zhu, J. Y.; Mao, Z. W.; Gao, C. Y. Adsorption of plasma proteins and fibronectin on poly(hydroxylethyl methacrylate) brushes of different thickness and their relationship with adhesion and migration of vascular smooth muscle cells. *Regen. Biomater.* **2014**, *1*, 17−25.
(55) Kashiwagi, T.; Ito, Y.; Imanishi, Y. Synthesis and Non-thrombogenicity of Fluoroalkyl Polyetherurethanes. *J. Biomater. Sci., Polym. Ed.* **1994**, *5*, 157−166.
(56) Laupland, K. B.; Gregson, D. B.; Church, D. L.; Ross, T.; Pitout, J. D. D. Incidence, risk factors and outcomes of Escherichia coli bloodstream infections in a large Canadian region. *Clin. Microbiol. Infect.* **2008**, *14*, 1041−1047.
(57) Castro, C. I.; Briceno, J. C. Perfluorocarbon-Based Oxygen Carriers: Review of Products and Trials. *Artif. Organs* **2010**, *34*, 622−634.
(58) Clark, L. C.; Becattini, F.; Kaplan, S.; Obrock, V.; Cohen, D.; Becker, C. Perfluorocarbons Having a Short Dwell Time in Liver. *Science* **1973**, *181*, 680−682.

DOI: 10.1021/acsami.5b05865
ACS Appl. Mater. Interfaces 2015, 7, 19466−19473